The retinoid-related orphan receptor alpha is essential for the end-stage effector phase of experimental epidermolysis bullosa acquisita

Hengameh Sadeghi, Yask Gupta, Steffen Moeller, Unni K. Samavedam, Martina Behnen, Anika Kasprick, Katja Bieber, Susen Mueller, Kathrin Kalies, Andreia de Castro Marques, et al.

The retinoid-related orphan receptor alpha is essential for the end-stage effector phase of experimental epidermolysis bullosa acquisita

Hengameh Sadeghi,[1] Yask Gupta,[1] Steffen Möller,[1] Unni K Samavedam,[1] Martina Behnen,[2] Anika Kasprick,[1] Katja Bieber,[1] Susen Müller,[1] Kathrin Kalies,[3] Andreia de Castro Marques,[1] Andreas Recke,[1] Enno Schmidt,[1] Detlef Zillikens,[1] Tamás Laskay,[2] Jean Mariani,[4,5] Saleh M Ibrahim[1†] and Ralf J Ludwig[1†*]

[1]Department of Dermatology, University of Lübeck, Germany
[2]Institute for Medical Microbiology and Hygiene, University of Lübeck, Germany
[3]Institute of Anatomy, University of Lübeck, Germany
4Sorbonne Universités, UPMC Univ Paris 06, UMR 8256 B2A Biological Adaptation and Ageing, Paris, France
[5]CNRS, UMR 8256 B2A Biological Adaptation and Ageing, Paris, France

*Correspondence to: Ralf J Ludwig, MD, Department of Dermatology, University of Lübeck, Ratzeburger Allee 160, D-23538 Lübeck, Germany. E-mail: ralf.ludwig@uksh.de

† These authors contributed equally to this study.

Genetic studies have added to the understanding of complex diseases. Here, we used a combined genetic approach for risk-loci identification in a prototypic, organ-specific, autoimmune disease, namely experimental epidermolysis bullosa acquisita (EBA), in which autoantibodies to type VII collagen (COL7) and neutrophil activation cause mucocutaneous blisters. Anti-COL7 IgG induced moderate blistering in most inbred mouse strains, while some showed severe disease or were completely protected. Using publicly available genotyping data, we identified haplotype blocks that control blistering and confirmed two haplotype blocks in outbred mice. To identify the blistering-associated genes, haplotype blocks encoding genes that are differentially expressed in EBA-affected skin were considered. This procedure identified nine genes, including *retinoid-related orphan receptor alpha* (*RORα*), known to be involved in neurological development and function. After anti-COL7 IgG injection, RORα+/− mice showed reduced blistering and homozygous mice were completely resistant to EBA induction. Furthermore, pharmacological RORα inhibition dose-dependently blocked reactive oxygen species (ROS) release from activated neutrophils but did not affect migration or phagocytosis. Thus, forward genomics combined with multiple validation steps identifies RORα to be essential to drive inflammation in experimental EBA.

Keywords: skin; autoimmunity; neutrophil; RORα; animal models; modulation

Introduction

Autoimmune disorders are examples of complex diseases and have become a major health burden over the last decades [1]. These diseases are characterized by an aberrant immune response against self-antigens [2], and treatment most commonly relies on general immunosuppression. Although in most cases, treatment controls symptoms, it rarely leads to complete remission [3]. The overall increased mortality in these patients may further increase with a higher degree of immunosuppressive treatment [4]. Therefore, the medical need to develop novel treatment strategies for autoimmune diseases is currently unmet. One possible approach to identify potential pathways for pharmacological modulation is the identification of genetic susceptibility loci. Proof-of-concept studies have demonstrated that human genetics can be used to guide the development of phenotype-based, high-throughput, small-molecule screens to identify potential novel therapies for autoimmune diseases such as rheumatoid arthritis [5]. The, albeit independent, identification of risk loci in the TNFα, p40, and IL-17 pathways in psoriasis, which is a chronic inflammatory skin disease, and the effective treatment of psoriasis using the respective biologicals [6] underscore the potential of genetic studies to identify novel therapeutic targets to treat complex diseases.

However, in humans and experimental animal models, genetic studies are expensive and time-consuming. In addition, the pathogenesis of autoimmune diseases is complex and characterized by multiple steps and molecular pathways that are involved in the generation

of an autoimmune response (afferent immune phase) that translates into tissue damage (effector inflammatory phase) as well as the persistence of immune and inflammatory responses over time. This multiplicity of events reads out as complex inheritance patterns, lowers the signal-to-noise ratios in the analyses, and generally hinders our progression towards identifying heritable influences [7]. Genetic analyses of animal models of autoimmunity could be clarified by separately viewing distinct disease phases.

To address this, we used a model of antibody transfer-induced epidermolysis bullosa acquisita (EBA) combined with a novel approach to identify susceptibility genes of autoantibody-induced blistering. EBA is a prototypical, organ-specific autoimmune disease that is clinically characterized by chronic, subepidermal (muco)-cutaneous blistering [3]. Type VII collagen (COL7) has been identified as the autoantigen in EBA [8], and the induction of blister formation by anti-COL7 antibodies has been demonstrated *in vitro* and *in vivo* [9]. In EBA pathogenesis, two major pathways can be distinguished. The disease is initiated by the CD4-dependent formation of IgG autoantibodies directed against COL7 [10]. Subsequently, in the effector phase of EBA, these autoantibodies form immune complexes at the dermal–epidermal junction, which lead to blistering. These later events can be investigated in antibody-transfer models, while the events leading to autoantibody production are duplicated in immunization-induced model systems [9].

We previously demonstrated associations between immunization-induced EBA and the H2s haplotype as well as several quantitative trait loci (QTL) outside of the MHC locus [9]. This finding was in line with observations in EBA patients, in whom associations with the MHC locus, as well as an overrepresentation of black patients, have been described [11,12]. These genetic risk loci comprise several hundreds of genes, and as detailed above, these data do not allow for distinguishing between risk alleles for disease induction and those associated with autoantibody-mediated skin blistering. To address this, we aimed to identify novel genetic risk genes that are associated with anti-COL7-induced skin blistering. First, experimental EBA was induced in 18 different inbred mouse strains, which showed high variability in clinically manifested subepidermal blistering. This phenotypic trait in inbred mouse strains was then correlated with publicly available genotyping data using forward genomics, which led to the identification of nine loci that were associated with clinical EBA severity. Two of these loci were confirmed in over 300 mice from an advanced intercross mouse line (AIL) [13]. Of these genes, only those that showed altered expression in skin affected by experimental EBA were considered further. Ultimately, one of the nine candidate genes was tested in the respective knock-out mouse strain, which led to the identification of RORα. To determine whether RORα is also involved in the activation of human neutrophils, the effect of pharmacological RORα blockade on the activation of isolated human neutrophils was evaluated.

Materials and methods

Studies involving human material

Approval for studies using biological material from humans was obtained from the Institutional Review Board at the University of Lübeck (Lübeck, Germany; AZ 09–140) and written informed consent was obtained, as outlined in the Declaration of Helsinki.

Mice

Mice from inbred mouse strains (A/J, AKR/J, B10.S-H2s/SgMcdJ, BALB/cJ, BXD2/TyJ, C3H/HeJ, C57Bl/6J, Cast/EiJ, CBA/J, DBA1/J, FVB/NJ, MRL/MpJ, NOD/ShiLtJ, NZM2410/J, PL/J, PWD/PhJ, SJL/J, and WSP/EiJ) were obtained from The Jackson Laboratory (Bar Harbor, Maine, USA). Mice of the sixth generation of a recently described, autoimmune-prone advanced intercross line (AIL) were generated as described elsewhere [13]. In brief, parental mouse strains (MRL/MpJ, NZM2410/J, BXD2/TyJ, and Cast/EiJ) were intercrossed at an equal strain and sex distribution. The parental origin of generation 1 (G1) offspring mice was considered when setting up mating for the generation of G2 mice to maintain an equal distribution of the original strains. This procedure was also followed for intercrossing G2 mice. At least 50 breeding pairs were used as parents for the next generation of mice. RORα-deficient mice were generated as described previously [14]. With the exception of RORα-deficient mice, mice aged 6–8 weeks were used for the experiments. For experiments with RORα-deficient mice, animals aged 2–3 weeks were used. All animals were housed in specific pathogen-free conditions and fed standard mouse chow and acidified drinking water *ad libitum*. All clinical examinations, biopsies, and bleedings were performed under anaesthesia using intraperitoneal (i.p.) administration of a mixture of ketamine (100 μg/g) and xylazine (15 μg/g). Animal experiments were approved by the local authorities of the Animal Care and Use Committee (Kiel, Germany; AZ 78-5/12) and performed by certified personnel.

Induction of experimental EBA and clinical evaluation

Experimental EBA was induced by anti-COL7 IgG transfer into mice as described previously [15]. Disease severity is expressed as the percentage of body surface area that was affected by skin lesions and was determined 2, 4, 8, and 12 days after the first IgG injection. From these data, the area under the curve, as a cumulative score of clinical disease taking both onset and maximum severity into account, was calculated for each individual mouse. Blood and tissue samples were collected on day 12. Mice were then examined for their general condition and for evidence of cutaneous lesions (ie erythema, blisters, erosions, alopecia, and crusts) every fourth day for 12 days.

Treatment of mice with SR3335

The effects of the inverse RORα agonist on blistering in experimental EBA and bullous pemphigoid (BP) were investigated by local injection of either rabbit anti-COL7 (EBA) or anti-COL17 (BP) IgG as described previously [16,17] with minor modifications. In brief, 0.7 mg of rabbit anti-mouse COL7 IgG or 2 mg of rabbit anti-mouse COL17 IgG diluted in PBS to a final volume of 50 µl was injected once intradermally (i.d.) in the base of the ear. This dosing was selected as this induced moderate disease, determined in preceding dose-finding experiments of this particular immune-IgG batch (data not shown). RORα was blocked during the entire experiment by administering the inverse agonist SR3335 (30 mg/kg body weight; Cayman Chemical, Ann Arbor, MI, USA) or DMSO (treatment control) twice per day starting 24 h before antibody injection. Endpoints included measurement of ear thickness (using a spring-loaded micrometer; Mitutoyo, Neuss, Germany) and scoring of the percentage of affected area at the ears.

Genotyping

Single-nucleotide polymorphism (SNP) genotyping

DNA was extracted from mice tail biopsies using a DNeasy® Blood & Tissue kit (Qiagen, Hilden, Germany) according to the manufacturer's instructions. For the genotyping of SNPs (rs27019283, rs29179064, rs4212464, rs33217114, rs29543297, rs31459209, rs30860794, rs1479871, and rs13480247), the TaqMan® SNP Genotyping Assay (Applied Biosystems, Foster City, CA, USA) was used. The amplification mixtures included 10 ng of DNA, 1× TaqMan® Genotype PCR Master Mix (Applied Biosystems), the 1× TaqMan® SNP Genotyping Assay (Applied Biosystems) including an allele-specific probe and primers that were labelled with the two allele-specific fluorescent reporter dyes VIC and FAM (Supplementary Table 1), and Milli-Q water in a 12-µl reaction. The PCR reactions were performed using Realplex and 96-well plates. The PCR profile was as follows: samples were heated for 10 min at 95°C and amplified for 40 cycles of 15 s at 95°C and 1 min at 60°C; two negative controls were included on each plate.

RORα genotyping

DNA was extracted from tail biopsies using a DNeasy® Blood and Tissue kit (Qiagen). PCR was performed in a total reaction volume of 20 µl that contained 0.2 µl of each primer (10 µM), 60 ng of DNA, and 1.25 µl of 5× Phusion HF Buffer. The samples were heated for 5 min at 94°C and amplified for 40 cycles of 30 s at 94°C, 30 s at 53°C, and 30 s at 72°C, and finally at 72°C for 10 min. The primers used were as follows: ROR S: 5′-TTCAGGAGAAGTCAGCAGAGC-3′; ROR As: 5′-TCACCGGCTAGTTGGCTGATTCC-3′; and Bgal As: 5′-TGTGAGCGAGTAACAACCCGTCGGATT CT-3′ (Biomers, Ulm, Germany). The PCR products were separated using 2% agarose gel electrophoresis, stained with SYBR Green (Qiagen), and photographed under UV light. WT (wild-type) samples should result in a product of approximately 318 bp, and ROR-Bgal samples should result in a band of 450 bp.

Histology

H&E staining and direct and indirect immunofluorescence (IF) microscopy were performed as described previously [15].

In vitro neutrophil activation

Heparin-anticoagulated blood was drawn from healthy volunteers using venipuncture. Polymorphonuclear leukocytes (granulocytes) were isolated using Polymorphprep or Percoll according to the manufacturer's instructions. For *in vitro* studies with the inverse RORα agonist SR3335, stock solutions were prepared in DMSO before every use and diluted with appropriate medium as used in the assays to final concentrations of 0.1, 1, 10 or 100 µM (0.1% v/v DMSO). Isolated cells were pre-incubated with SR3335 for 15 min at 37°C prior to activation by immune complexes. DMSO-treated and untreated cells served as controls. Immune complexes were generated by incubation of either a recombinant fragment of COL7 [18] or human serum albumin (HSA) with a corresponding monoclonal IgG1 antibody. The luminol (5-amino-2,3-dihydro-1,4-phthalazinedione)-amplified chemiluminescence assay was used to measure the release of ROS, which served as a measure of neutrophil activation [19]. To analyse the effect of DMF on neutrophil chemotaxis, a modified chemotaxis assay was performed using a 24-well transwell system with 3-µm pore filters (Costar, Bodenheim, Germany) as described previously [20]. To evaluate phagocytic activity, freshly isolated, viable neutrophils were stimulated with 100 ng/ml LPS and 200 U/ml IFNγ. Thereafter, FluoSpheres carboxylate-modified microspheres (Invitrogen, Carlsbad, CA, USA) were added, and subsequent phagocytosis of the yellow-green fluorescent FluoSpheres by neutrophils was assessed using flow cytometry (FACSCalibur, BD) and fluorescence microscopy (Axioskop 40, Zeiss) of Giemsa-stained cytocentrifuge slides. In control samples, phagocytosis was inhibited by 10 µg/ml cytochalsin D.

Statistical analysis

Whole-genome genotyping data were collected from the Sanger Center (http://www.sanger.ac.uk/resources/mouse/genomes) and The Jackson Laboratory (http://phenome.jax.org). SNPs from the same strain with conflicting information between these sources were removed using R (http://www.r-project.org). Single SNP association tests were performed using PLINK, and haplotypes were investigated using Haploview [21]. Genotyping data from the selected SNPs that were evaluated in animals from the advanced intercross line

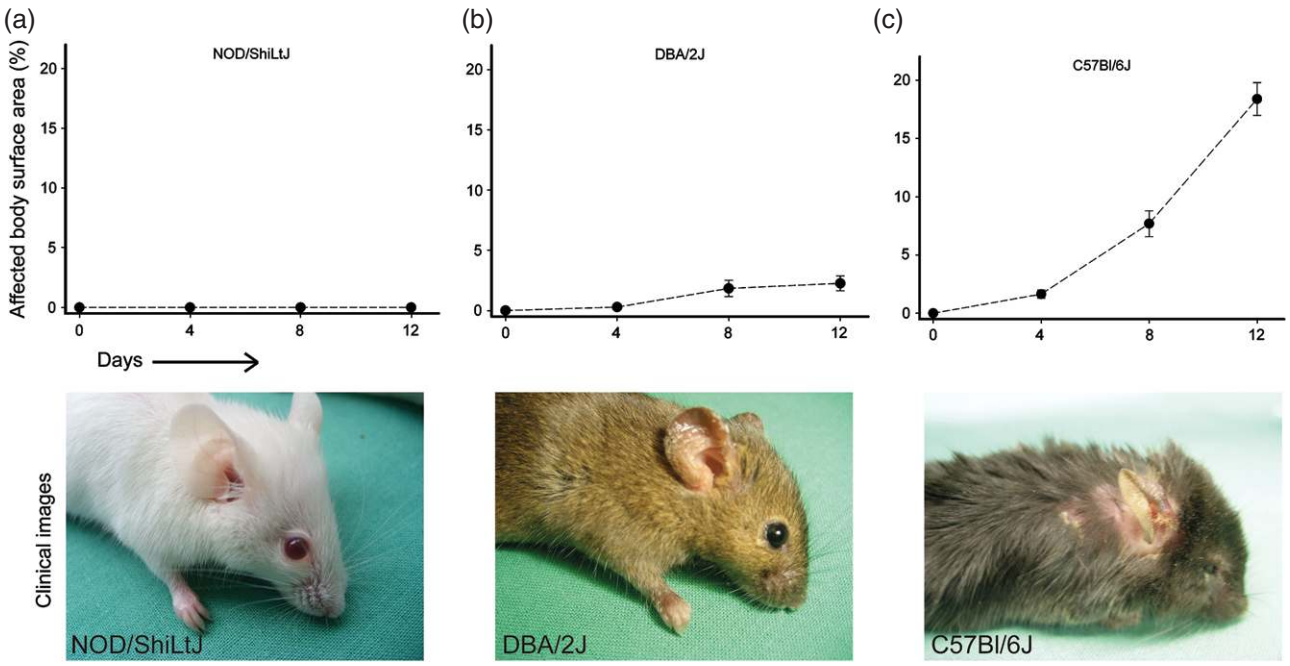

Figure 1. Induction of experimental EBA by anti-COL7 IgG transfer in mice is strain-dependent. Disease score expressed as the percentage of body surface area affected by skin lesions during an observation period of 12 days in (a) NOD/ShiLtJ (resistant), (b) DBA/2J (mild disease), and (c) C57Bl/6J (severe EBA) mice injected with anti-COL7 IgG. Below: representative clinical pictures of one mouse of the indicated strains obtained at day 12 of the experiment.

were analysed using ANOVA on linear models, with the maximum disease score as the dependent variable and SNP data and the gender of the animals as covariates. Each SNP was analysed separately. The obtained p values were corrected using the Benjamini–Hochberg method, and all calculations were performed using GNU R with standard base and stats packages [22]. To determine differentially expressed genes in the skin of mice with evident blistering after the transfer of anti-COL7 IgG compared with mice injected with control IgG, a previously published dataset was used [23]. From these datasets, all genes with a two-fold or greater change in expression that were expressed by the regions characterized by the SNP in the validation experiment were considered. Comparisons or differences in the extent of clinical phenotypes were performed using SigmaPlot (Version 12, Systat Software Inc, Erkrath, Germany). The tests used are indicated in the legends of the figures and tables. A p value less than 0.05 was considered significant.

Table 1. Clinical characteristics of antibody transfer-induced EBA in different strains of mice

Strain	Disease incidence	Onset day*	Maximum score*
NOD/ShiLtJ†	0/5	N/A	N/A
FVB/NJ†	2/5	8.0 ± 0.0	0.1 ± 0.1
A/J†	3/5	8.0 ± 0.0	0.5 ± 0.3
SJL/J†	3/6	8.0 ± 0.0	0.8 ± 0.1
MRL/MpJ‡	6/6	7.3 ± 1.6	1.3 ± 0.1
C3H/HeJ†	5/5	5.6 ± 3.6	1.4 ± 1.5
DBA/1J†	6/6	6.7 ± 3.3	2.3 ± 1.5
NZM2410/J†‡	5/5	7.2 ± 1.8	2.4 ± 0.7
PL/J†	5/5	4.0 ± 0.0	6.0 ± 0.5
AKR/J†	5/5	4.8 ± 1.8	6.9 ± 2.5
BALB/cJ†	6/6	6.0 ± 2.2	10.3 ± 1.6
PWD/PhJ	4/4	5.0 ± 2.0	10.8 ± 3.8
CBA/J†	5/5	3.6 ± 0.9	11.5 ± 3.7
BXD2/TyJ ‡	6/6	4.0 ± 0.0	16.2 ± 5.1
C57Bl/6J†	11/11	3.3 ± 1.0	18.4 ± 4.7
B10.S-H2s/SgMcdJ	5/5	4.0 ± 0.0	19.2 ± 1.6
WSB/EiJ†	4/4	2.0 ± 0.0	7.8 ± 0.6§
Cast/EiJ†‡	5/5	2.4 ± 0.9	10.0 ± 3.4‖

*Calculated for diseased mice only.
†Used for forward genetic analysis.
‡Used for intercrossing to generate AIL mice.
§One mouse died 2 days after the first IgG injection and another mouse died on day 4. The indicated scores correspond to those obtained in the two surviving mice on day 12.
‖Maximum disease was reached on day 8; thereafter, all mice died.
N/A = not applicable.

Results

Induction of skin blistering in experimental EBA by antibody transfer is strain-dependent

Previous work demonstrated a strain dependency of antibody-induced nephritis [24] and arthritis [7]. The clinical diversity among the 18 inbred mouse lines analysed here confirms the findings of the strain dependency of antibody transfer-induced inflammatory disease mouse models. In detail, NOD/ShiLtJ, FVB/NJ, A/J, SJL/J, and MRL/MpJ were among the resistant strains, whereas BXD2/TyJ, C57Bl/6J, B10.S-H2s/SgMcdJ, and Cast mice were highly susceptible to antibody transfer-induced EBA (Figure 1 and Table 1).

Table 2. Single-nucleotide polymorphisms (SNPs) for antibody-induced skin blistering in experimental EBA that were identified using forward genomics

Block (#: bp)*	SNP ID†	Chr	Position (bp)†	MAF	Alleles major (minor)	Estimate ± SD‡	Unadj p§	Adj p‖
A: 34019743 – 89135715	rs31459209	1	34019743	0.43	C (T)	0.03 ± 0.44	0.9499	0.9499
B: 73683457 – 90622796	rs30860794	6	74799493	0.20	C (T)	0.32 ± 0.62	0.6052	0.7565
C: 87192012 – 87908605	rs13479871	8	87590219	0.18	A (G)	0.44 ± 0.73	0.5481	0.7565
D: 61628273 – 85033289	***rs13480247***	***9***	***65394049***	***0.09***	***C (A)***	***−2.40 ± 1.14***	***0.0360***	***0.1799***
E: 62666281 – 110131804	rs27019283	11	110131804	0.21	A (C)	0.80 ± 0.57	0.1608	0.5359
F: 92019623 – 94457772	rs29179064	12	92019623	0.18	C (T)	−0.16 ± 0.54	0.7631	0.8479
G: 85623259 – 98046063	rs4212464	16	85633259	0.35	T (C)	0.51 ± 0.49	0.2969	0.5939
H: 24184758 – 26451588	rs33217114	17	26451588	0.35	G (A)	0.48 ± 0.44	0.2678	0.5939
I: 57559944 – 57589991	***rs29543297***	***18***	***57589991***	***0.47***	***G (A)***	***1.98 ± 0.48***	***0.0001***	***0.0005***

Haplotype blocks highlighted in bold and italic indicate those that were used for further investigations.
*Blocks detected using forward genomics.
†SNPs selected for individual blocks and location, NCBI build 37.
‡Coefficient of minor allele counts in a linear model for maximum disease score, which included mouse gender as a second covariate.
§Unadjusted p values for ANOVA of linear models.
‖Adjusted p values, Benjamini–Hochberg method.
Chr = chromosome; MAF = minor allele frequency.

Forward genomics identifies susceptibility loci for antibody-induced skin blistering in experimental EBA

We then used forward genetics to examine the possible genetic mechanism of antibody transfer-induced EBA in mice. The data from 14 of the 18 mouse strains injected with anti-COL7 IgG, shown in Table 1, were included in this analysis. This approach resembles the differential analysis for disease susceptibility across human ethnic groups [25]. The top-scoring single-nucleotide polymorphisms (SNPs) from the association study of the most versus the least susceptible strains are displayed in Table 2. These best-performing SNPs were used as tags for haplotype blocks for further investigation.

Confirmation of rs29543297 in an autoimmune-prone advanced intercross mouse line (AIL) as a susceptibility locus for skin blistering in experimental EBA

To validate the above-identified loci, we induced EBA in genetically diverse AIL mice [13]. In detail, 315 mice of the sixth generation (G6) were injected with anti-COL7 IgG and 310 mice were included in the analysis. The remaining five animals died before the last day of the experiment. Overall, 87% of the mice developed clinical lesions and 13% were resistant to disease induction (Figure 2). EBA onset was observed 4 ± 2.3 days after the initial anti-COL7 IgG injection, and the mean maximal disease severity, which is expressed as the affected body surface area, was $6.0 \pm 5.2\%$. Compared with female mice, the extent of skin blistering was significantly lower in males ($p = 0.043$). Other phenotypic traits, such as weight and fur colour, had no impact on clinical EBA manifestation (not shown). Subsequently, all 310 of these mice were genotyped using markers that distinguished the nine identified haplotype blocks. In this analysis, we confirmed associations between skin blistering induced by the transfer of anti-COL7 IgG and rs13480247 and rs29543297. However, after adjustment of the p values, only rs29543297 remained significant (Table 2). Given the restricted population size, we also included the haplotype block represented as rs13480247, which had the second-best p value. All other SNPs that were used to validate the identified regions could not be confirmed in AIL mice (Table 2).

Expression profiling to decrease the number of potential susceptibility genes

To identify the genetic control of antibody-induced skin blistering at the single-gene level, we examined the correlations between previous expression profiling data that were obtained from the skin of mice with experimental EBA [23] and genes encoded by 9:61628273–85033289 and 18:57559944–57589991 (blocks D and I from Table 2). Based on expression profiling, genes showing a greater than two-fold change in expression in the skin of mice with EBA compared with healthy control mice were considered. This led to the identification of nine genes encoded by 9:61628273–85033289 and 18:57559944–57589991 (Table 3).

Identification of the retinoid-related orphan receptor alpha (RORα) as a risk gene for antibody-induced tissue damage in experimental EBA

Among these genes, *ROR*α was selected for further validation because (i) it showed the highest fold change in our expression profiling data; (ii) RORα-deficient mice were available [14]; (iii) the gene is polymorphic in EBA-resistant and -susceptible strains (Supplementary Table 2); and (iv) combined pharmacological blockade of RORα and RORγ prevented the induction of experimental autoimmune encephalomyelitis [26]. In other models of inflammatory disease, RORα was required for the generation of natural helper lymphoid cells and the subsequent induction of allergic lung inflammation [27] and (together with RORγ) Th lineage differentiation [28]. The transfer of anti-COL7 IgG into RORα heterozygous (+/−) and wild-type littermate controls (+/+) resulted in a significant reduction in

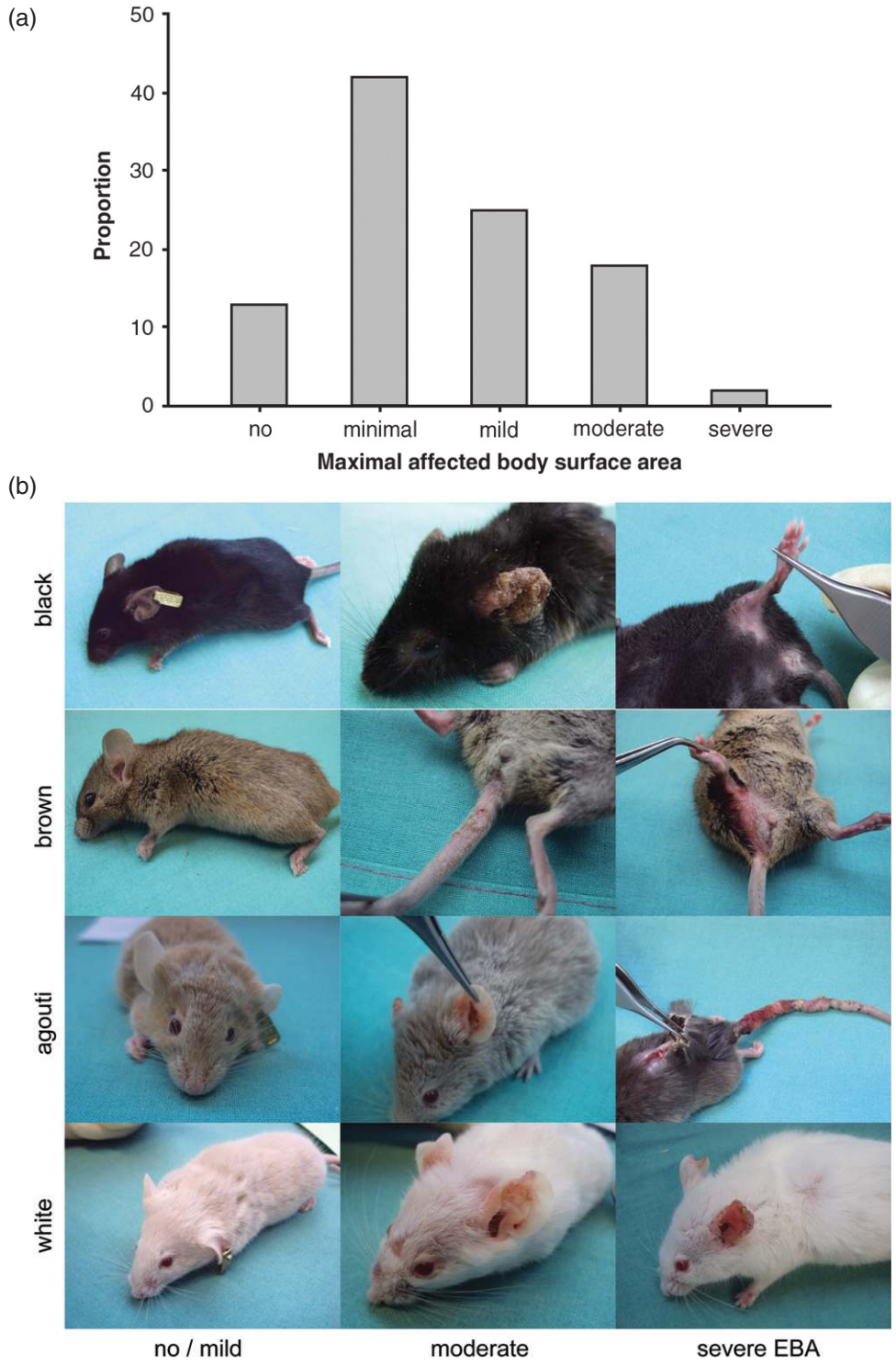

Figure 2. Mice of an autoimmune-prone advanced intercross mouse line (AIL) show high variation in susceptibility to antibody transfer-induced EBA. (a) Experimental EBA was induced by anti-COL7 IgG transfer in mice from an autoimmune-prone advanced intercross mouse line (AIL). Most mice developed clinically manifest blistering. The graph shows the proportion of mice with no, minimal, mild, moderate or severe skin blistering, which corresponded to percentages of the body surface area affected by skin blistering of <1%, 1–4.9%, 5–9.9%, 10–20% or >20%, respectively. (b) Representative clinical photographs of differently coloured AIL mice showing the no, moderate, and severe skin blistering phenotypes.

neutrophil-dependent skin blistering in RORα +/− mice. The cumulative disease activity was reduced from 58.0 ± 3.1 in RORα +/+ mice to 42.8 ± 3.5 in RORα +/− mice (Figures 3a–3d). To test whether the complete absence of RORα has a more pronounced effect on blister manifestation in experimental EBA, anti-COL7 IgG was injected into two 2-week-old RORα −/− mice. This early time point was selected because RORα −/− mice did not survive beyond 5–6 weeks. RORα +/+ littermates of the same age were used as controls. In all of the latter animals, anti-COL7 IgG induced subepidermal blistering that was associated with IgG and C3

Table 3. Differently expressed genes within 9:61628273–85033289 and 18:57559944–57589991

Gene		Probe set	Entrez gene	Fold change
Car12	Carbonic anhydrase 12	1428485_at	76459	3·11
Clpx	Caseinolytic peptidase X (*E. coli*)	1439342_at	270166	−5·46
Ccnb2	Cyclin B2	1450920_at	12442	2·77
Igdcc3	Immunoglobulin superfamily, DCC subclass, member 3	1423496_a_at	19289	4·19
Rora	RAR-related orphan receptor alpha	1443647_at	19883	6·15
		1457177_at	19883	−5·12
		1458129_at	19883	−5·33
		1436326_at	19883	−3·37
Sltm	SAFB-like, transcription modulator	1456683_at	66660	−2·43
Rfx7	Regulatory factor X, 7	1440068_at	319758	−4·12
		1460567_at	319758	−2·79
Zfp280d	Zinc finger protein 280 D	1426556_at	235469	−2·82
Tcf12	Transcription factor 12	1439619_at	21406	−4·85

deposition along the dermal–epidermal junction (Figure 3e). In contrast, RORα −/− mice were completely protected from anti-COL7 IgG-induced skin blistering, despite the presence of similar IgG and C3 deposition along the dermal–epidermal junction (Figure 3e). To further validate the contribution of RORα in this model, we next treated C57Bl/6 mice with the inverse RORα agonist SR3335 and simultaneously induced a localized form of EBA by intradermal injection of anti-COL7 into the ears. In line with the data obtained in RORα-deficient and -heterozygous mice, pharmacological RORα inhibition also impaired blistering in experimental EBA (Figure 4). Similar observations were made in a model of antibody transfer-induced BP (Figure 4). This indicates that effector mechanisms downstream of IgG binding and complement activation are mediated by RORα.

In human neutrophils, immune complex-induced ROS release requires RORα

RORα has been documented in human and murine neutrophils [29,30]. Our findings demonstrate a complete dependency of blister induction on RORα in experimental EBA (Figure 3), which also requires the presence of Gr-1+ myeloid cells [9]. Hence, we hypothesized that RORα is involved in the regulation of neutrophil activation by immune complexes. To challenge this assumption and translate our findings from mice to humans, human neutrophils were activated using immune complexes in the absence or presence of the inverse RORα agonist SR3335 [31]. When neutrophils were activated with immune complexes in the presence of SR3335, incomplete, but significant, inhibition of ROS release was observed at 100 μM (not shown). When pre-incubated with SR3335, complete inhibition of immune complex-induced ROS release was observed at doses ≥10 μM (Figures 5a and 5b). SR3335 had no effect on the TNFα- or IL-8-induced migration of human neutrophils (Figure 5c) or on the LPS/IFNγ-induced phagocytosis of fluorescently labelled beads (Figures 5d and 5e). The effects of SR3335 on human neutrophils were not due to any toxic effects, as the number of live cells after 1.5 or 4.0 h was not altered at any concentration used in this study when compared with the solvent (>97% viable cells in all conditions after 4 h of incubation).

Discussion

Collectively, applying forward genomics combined with validation using genotyping, expression profiling, and knock-out mice, we identified RORα as a regulator of antibody-induced tissue damage. RORα maps to a conserved region of homology on human chromosome 15q21–q22 and mouse chromosome 9 [32]. Although RORα is expressed in a variety of tissues, including immune cells, it is most highly expressed in the brain. Lack of RORα expression causes neurological symptoms, such as ataxia and severe cerebellar atrophy. Furthermore, RORα has been shown to contribute to retinal development, bone formation, circadian behaviours, lipid metabolism, and lymphocyte development [28,33,34], which results in the premature death of RORα-deficient mice [14]. In genome-wide association studies, RORα has been associated with predominant neurological disorders [35], C-reactive protein levels [36], the concentrations of liver enzymes in the plasma [37], and asthma [38]. In the immune system, RORα (together with RORγ) has been shown to modulate Th17 polarization [26] and nuocyte development [39]. However, it remains unclear whether the observed defective lymphocyte development in RORα-deficient mice is caused indirectly, ie by stress due to the movement incoordination experienced by these mice, or is the result of a neurological defect that results in abnormal hormone activities, affecting lymphocyte development [40].

Regarding neutrophils, a potential contribution of RORα to their (patho)-physiology has not been assessed. In an observational study, decreased *RORα* mRNA expression was noted in human volunteers who were administered a standard dose of endotoxin, and expression was inversely correlated with the release of pro-inflammatory cytokines [29]. In the present study, based on forward genomics combined with several validation steps, including the use of knock-out mice, we identified RORα as a requirement for the end-stage effector phase of experimental EBA. This effect is most

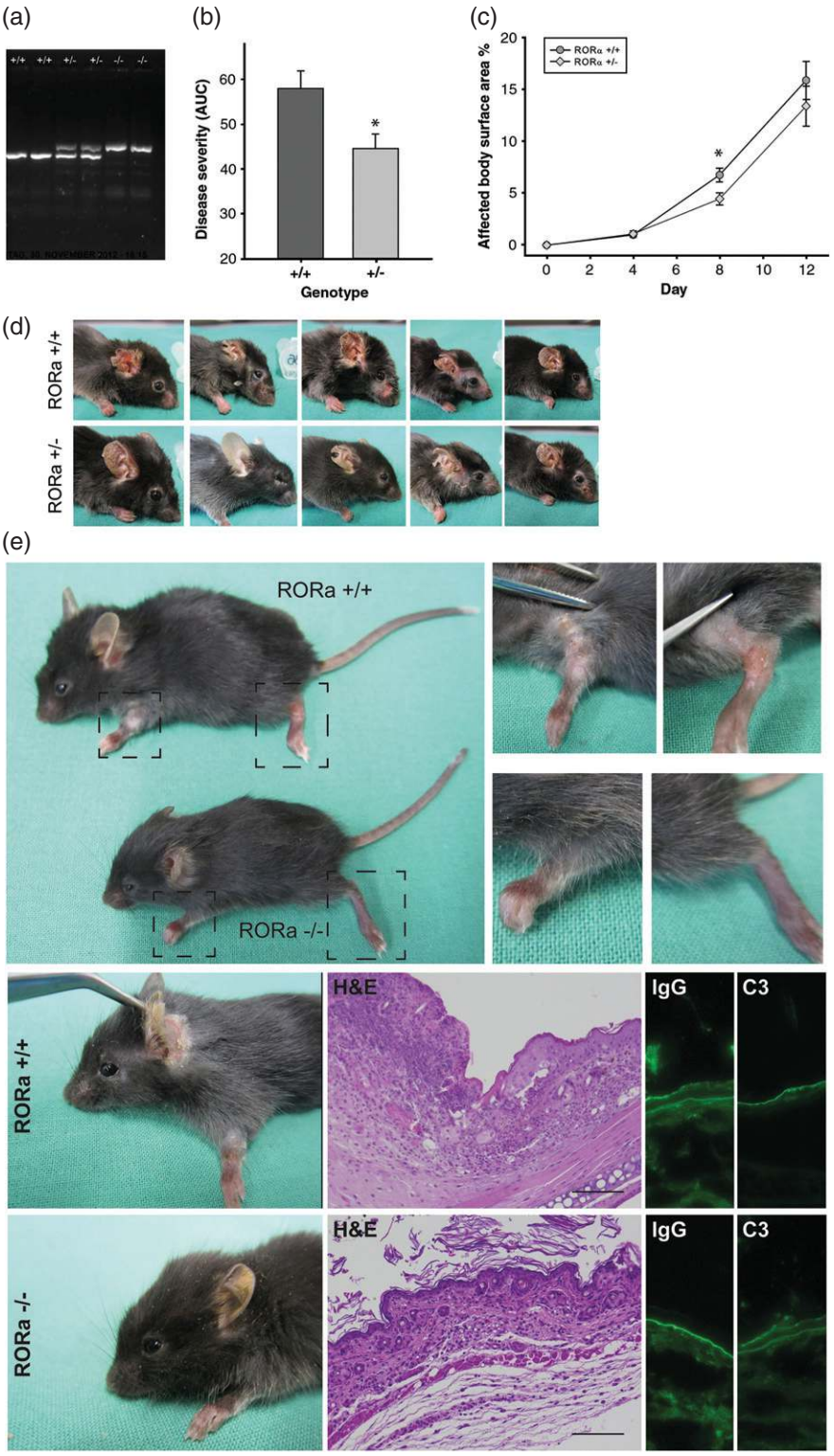

Figure 3. Combination of forward genetics, validation in AIL mice, and expression profiling identifies RORα as an EBA susceptibility gene. (a) Genotype of RORα +/+, +/− or −/− mice. (b) Compared with RORα +/+ mice ($n = 23$), RORα +/− mice ($n = 19$) showed less skin blistering after the transfer of anti-COL7 IgG. The cumulative clinical disease severity is expressed as the area under the curve (AUC), which was calculated using the individually affected body surface area on days 4, 8, and 12. *$p < 0.05$ (two-way ANOVA, considering gender and genotype as independent variables, and the Bonferroni t-test were used for multiple comparison procedures). (c) Here, the percentage of affected body surface area from panel b is plotted against time. Overall, RORα mice showed less blistering on day 8 of the experiment. The difference observed at day 12 was not statistically significant (*$p < 0.05$, rank-sum test). (d) Representative clinical photographs of anti-COL7 IgG-injected RORα +/+ and +/− mice on day 12 of the experiment. (e) Two- to three-week-old mice were injected with anti-COL7 IgG. Clinical photographs (and details) of skin lesions in RORα +/+ and −/− mice, which demonstrate a lack of clinically evident blistering in RORα −/− mice. In line with the clinical observations, histological examination of RORα −/− skin obtained on day 8 after the first anti-COL7 IgG injection showed no presence of subepidermal blistering and the absence of a dermal leukocyte infiltrate (bar corresponds to 100 μm). No differences in IgG and C3 deposition along the dermal–epidermal junction were observed.

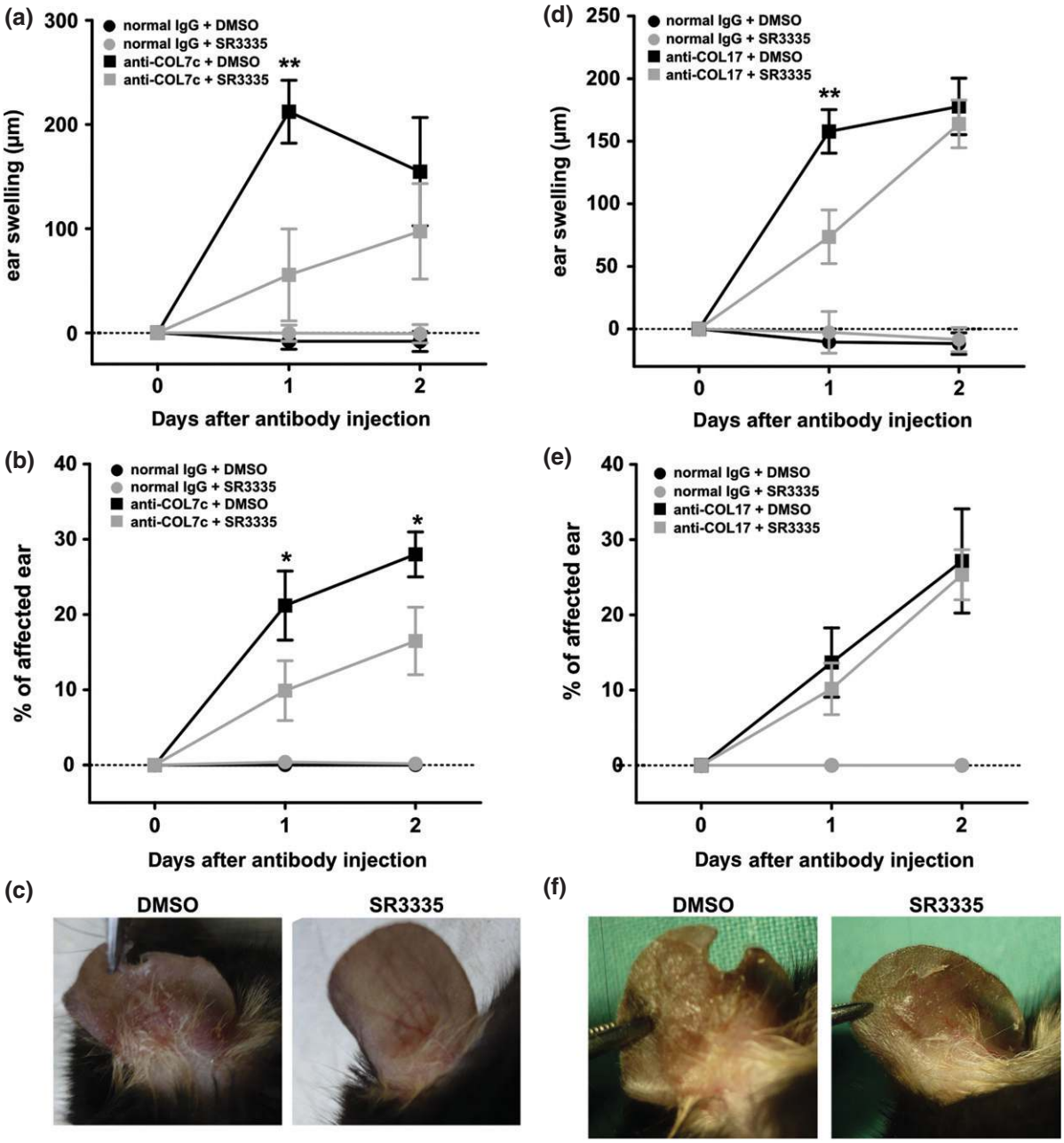

Figure 4. The inverse RORα agonist SR3335 impairs blister formation in both antibody transfer-induced EBA and bullous pemphigoid (BP). Experimental EBA was induced in C57BL/6 mice ($n = 5$ per group) by a single intradermal injection of anti-COL7 IgG into the ear and disease development was observed over a period of 48 h. RORα was blocked during the entire experiment by administering the inverse agonist SR3335 (30 mg/kg body weight) or DMSO (treatment control) twice per day starting 24 h before antibody injection. Pharmacological blockade of RORα by SR3335 (a) delayed ear swelling as a measure of inflammation and (b) significantly reduced disease severity. (c) Representative clinical photographs of anti-COL7 IgG-injected and SR3335- or DMSO-treated mice on day 2 of the experiment. In a second set of experiments, experimental BP was induced in C57BL/6 mice ($n = 5$ per group) by a single intradermal injection of anti-COL17 IgG into the ear and disease development was observed over a period of 48 h. RORα was blocked during the entire experiment by administering the inverse agonist SR3335 (30 mg/kg body weight) or DMSO (treatment control) twice per day starting 24 hours before antibody injection. Pharmacological blockade of RORα by SR3335 (d) delayed ear swelling as a measure of inflammation but (e) had no impact on skin blistering. (f) Representative clinical photographs of anti-COL17 IgG-injected and SR3335- or DMSO-treated mice on day 2 of the experiment. Data are shown as mean ± SEM and statistically significant differences between SR3335- or DMSO-treated groups injected with anti-COL7 IgG were calculated using one-way ANOVA and the Bonferroni t-test for multiple comparison procedures.*$p < 0.05$; **$p < 0.01$.

likely mediated by the isoform detected by 1443647_at, because in contrast to the other RORα isoforms it shows enhanced expression in EBA and pharmacological inhibition of RORα hinders EBA induction. This indicates that RORα inhibition may have beneficial effects in neutrophil-dependent, chronic inflammatory diseases such as EBA [9], arthritis [41], and severe, neutrophil-dependent asthma [42]. By contrast, the blockade of RORα will most likely lead to defects in host defence. The risk/benefit ratio of targeting RORα in neutrophils must therefore be based on results from further experiments using additional model systems.

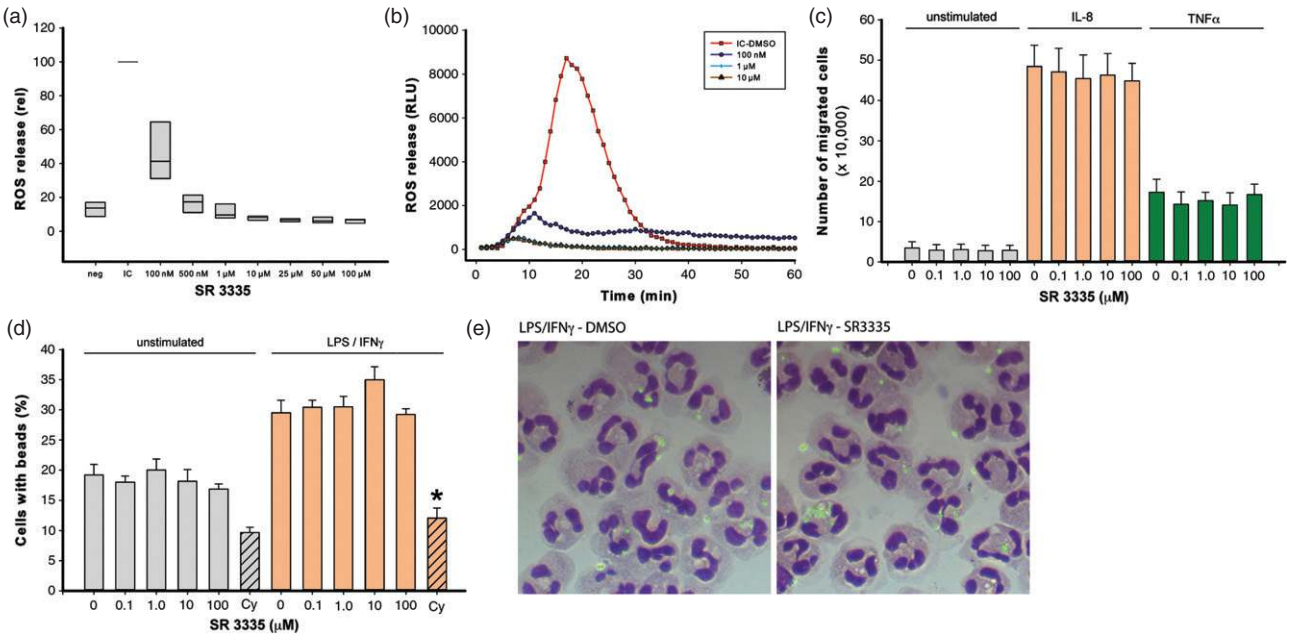

Figure 5. The inverse RORα agonist SR3335 inhibits immune complex-induced ROS release from human neutrophils. (a) Human neutrophils were activated by immune complexes in the absence or presence of SR3335. The release of reactive oxygen species (ROS) was used as a measure of neutrophil activation, which was dose-dependently inhibited by SR3335. The graph depicts normalized (immune complex-activated neutrophils) ROS release. Data are presented as the median (black line) and box plots (25/75-percentile) and are based on five different blood donors. $^*p < 0.05$ (ANOVA on ranks, with Dunn's method for multiple comparisons). (b) Representative ROS release from one experiment. (c) The effect of SR3335 on IL-8- or TNFα-induced migration of human neutrophils was evaluated. IL-8 and TNFα induced neutrophil migration ($p < 0.01$, t-test), and the addition of SR3335 had no effect on this cytokine-induced migration ($n = 3$ per group, ANOVA). (d) Phagocytosis of fluorescently labelled beads by LPS/IFNγ-activated neutrophils was also not affected by SR3335 (ANOVA, $n = 3$ per group). (e) Representative images of one experiment showing no difference in the accumulated green beads in neutrophils. Cy: Cytochalasin-D, used as a treatment control.

The end-stage effector phase of experimental EBA is initiated by the binding of anti-COL7 autoantibodies to their target antigen, which is located at the cutaneous basement membrane. This induces complement-, cytokine-, and integrin-dependent neutrophil extravasation into the skin [9,43,44]. In the skin, neutrophils bind to these immune complexes in an Fc gamma receptor IV-dependent manner [15,23,45]. Subsequently, a complex signalling cascade involving Akt, PI3K beta, MAPK1, and MAPK14 is initiated in neutrophils that ultimately leads to ROS and protease release, which has been demonstrated to cause blistering [16,46]. It is also conceivable that the receptor-associated protein tyrosine kinase Syk is required for neutrophil activation in EBA, because activating Fc gamma receptors, including Fc gamma receptor IV, activate Syk [47]. Regarding RORα-dependent signalling, it was shown that *RORα* influences genes involved in lipid and carbohydrate metabolism, cardiovascular and metabolic disease, LXR nuclear receptor signalling, and Akt and AMPK signalling in skeletal muscle [48,49]. In colon cancer, RORα inhibited canonical Wnt signalling [50]. Based on these findings and the observations that blistering in anti-COL7 transfer-induced EBA depends on neutrophils [51], it is feasible that RORα may modulate immune complex-induced signalling in neutrophils in this experimental model. A putative network of genes expressed in neutrophils known to contribute to blistering in EBA and genes controlled by RORα is shown in Supplementary Figure 1. Based on these data, RORα indirectly influences Akt signalling, which has been shown to contribute to immune complex-induced neutrophil activation [16]. Furthermore, RORα may also directly modulate Akt activity in immune cells, as described for RORα-regulated genes in skeletal muscle [48].

Our data demonstrate that forward genomics combined with validation using genotyping and expression profiling is a suitable approach for identifying susceptibility genes. The major advantages of this approach are the decreased expenditure and time required to identify novel risk genes for complex diseases. In contrast to GWASs or the classical mouse genomic tools that achieve similar goals, the approach described here is less standardized and, in addition to computational analysis, requires the input of hypothesis-based biological assumptions. Consequently, this approach is presumably more likely to miss associations; however, the false-positive detection rates should be similar for both approaches. Using this approach, RORα was identified to be essential for immune complex-mediated neutrophil activation and should be considered as a potential therapeutic target for the treatment of EBA and possibly other autoantibody-induced, neutrophil-mediated diseases, such as bullous pemphigoid and rheumatoid arthritis.

Acknowledgments

We thank Claudia Kauderer for providing excellent technical assistance. This study was supported, in part, by grants GRK 1727/1 (Research Training Group 'Modulation of Autoimmunity') and GRK1743/1 (Research Training Group 'Genes, Environment and Inflammation'), both from the Deutsche Forschungsgemeinschaft.

Author contribution statement

HS, UKS, MB, SM, AK, KB, KK, and ACM performed experiments. YG, SM, AR, and RJL did the statistical analysis. ES, DZ, TL, JM, and RJL wrote the manuscript. SMI and RJL designed the study. All of the authors were involved in data analysis and revisions of the manuscript.

References

1. Bach JF. The effect of infections on susceptibility to autoimmune and allergic diseases. *N Engl J Med* 2002; **347:** 911–920.
2. Rose NR, Bona C. Defining criteria for autoimmune diseases (Witebsky's postulates revisited). *Immunol Today* 1993; **14:** 426-430.
3. Schmidt E, Zillikens D. Pemphigoid diseases. *Lancet* 2013; **381:** 320–332.
4. Joly P, Roujeau JC, Benichou J, *et al.* A comparison of oral and topical corticosteroids in patients with bullous pemphigoid. *N Engl J Med* 2002; **346:** 321–327.
5. Li G, Diogo D, Wu D, *et al.* Human genetics in rheumatoid arthritis guides a high-throughput drug screen of the CD40 signaling pathway. *PLoS Genet* 2013; **9:** e1003487.
6. Reichert JM. Marketed therapeutic antibodies compendium. *MAbs* 2012; **4:** 413–415.
7. Ji H, Gauguier D, Ohmura K, *et al.* Genetic influences on the end-stage effector phase of arthritis. *J Exp Med* 2001; **194:** 321–330.
8. Woodley DT, Burgeson RE, Lunstrum G, *et al.* Epidermolysis bullosa acquisita antigen is the globular carboxyl terminus of type VII procollagen. *J Clin Invest* 1988; **81:** 683–687.
9. Ludwig RJ, Kalies K, Köhl J, *et al.* Emerging treatments for pemphigoid diseases. *Trends Mol Med* 2013; **19:** 501–512.
10. Iwata H, Bieber K, Tiburzy B, *et al.* B cells, dendritic cells, and macrophages are required to induce an autoreactive CD4 helper T cell response in experimental epidermolysis bullosa acquisita. *J Immunol* 2013; **191:** 2978–2988.
11. Gammon WR, Heise ER, Burke WA, *et al.* Increased frequency of HLA-DR2 in patients with autoantibodies to epidermolysis bullosa acquisita antigen: evidence that the expression of autoimmunity to type VII collagen is HLA class II allele associated. *J Invest Dermatol* 1988; **91:** 228–232.
12. Zumelzu C, Le Roux-Villet C, Loiseau P, *et al.* Black patients of African descent and HLA-DRB1*15:03 frequency overrepresented in epidermolysis bullosa acquisita. *J Invest Dermatol* 2011; **131:** 2386–2393.
13. Srinivas G, Möller S, Wang J, *et al.* Genome-wide mapping of gene–microbiota interactions in susceptibility to autoimmune skin blistering. *Nature Commun* 2013; **4:** 2462.
14. Steinmayr M, Andre E, Conquet F, *et al. staggerer* phenotype in retinoid-related orphan receptor alpha-deficient mice. *Proc Natl Acad Sci U S A* 1998; **95:** 3960–3965.
15. Sitaru C, Mihai S, Otto C, *et al.* Induction of dermal–epidermal separation in mice by passive transfer of antibodies specific to type VII collagen. *J Clin Invest* 2005; **115:** 870–878.
16. Hellberg L, Samavedam UK, Holdorf K, *et al.* Methylprednisolone blocks autoantibody-induced tissue damage through inhibition of neutrophil activation. *J Invest Dermatol* 2013; **133:** 2390–2399.
17. Kasprick A, Yu X, Scholten J, *et al.* Conditional depletion of mast cells has no impact on the severity of experimental epidermolysis bullosa acquisita. *Eur J Immunol* 2015; **45:** 1462–1470.
18. Recke A, Sitaru C, Vidarsson G, *et al.* Pathogenicity of IgG subclass autoantibodies to type VII collagen: induction of dermal–epidermal separation. *J Autoimmun* 2010; **34:** 435–444.
19. Yu X, Holdorf K, Kasper B, *et al.* FcγRIIA and FcγRIIIB are required for autoantibody-induced tissue damage in experimental human models of bullous pemphigoid. *J Invest Dermatol* 2010; **30:** 2841–2844.
20. Wilde I, Lotz S, Engelmann D, *et al.* Direct stimulatory effects of the TLR2/6 ligand bacterial lipopeptide MALP-2 on neutrophil granulocytes. *Med Microbiol Immunol* 2007; **196:** 61–71.
21. Barrett JC, Fry B, Maller J, *et al.* Haploview: analysis and visualization of LD and haplotype maps. *Bioinformatics* 2005; **21:** 263–265.
22. R Core Team. R: A Language and Environment for Statistical Computing. R Foundation for Statistical Computing: Vienna, 2013. Available from: http://www.R-project.org/
23. Kasperkiewicz M, Nimmerjahn F, Wende S, *et al.* Genetic identification and functional validation of FcγRIV as key molecule in autoantibody-induced tissue injury. *J Pathol* 2012; **228:** 8–19.
24. Xie C, Sharma R, Wang H, *et al.* Strain distribution pattern of susceptibility to immune-mediated nephritis. *J Immunol* 2004; **172:** 5047–5055.
25. Moller S, Koczan D, Serrano-Fernandez P, *et al.* Selecting SNPs for association studies based on population frequencies: a novel interactive tool and its application to polygenic diseases. *In Silico Biol* 2004; **4:** 417–427.
26. Solt LA, Kumar N, Nuhant P, *et al.* Suppression of TH17 differentiation and autoimmunity by a synthetic ROR ligand. *Nature* 2011; **472:** 491–494.
27. Halim TY, MacLaren A, Romanish MT, *et al.* Retinoic-acid-receptor-related orphan nuclear receptor alpha is required for natural helper cell development and allergic inflammation. *Immunity* 2012; **37:** 463–474.
28. Jetten AM. Retinoid-related orphan receptors (RORs): critical roles in development, immunity, circadian rhythm, and cellular metabolism. *Nucl Recept Signal* 2009; **7:** e003.
29. Haimovich B, Calvano J, Haimovich AD, *et al. In vivo* endotoxin synchronizes and suppresses clock gene expression in human peripheral blood leukocytes. *Crit Care Med* 2010; **38:** 751–758.
30. Werner JL, Gessner MA, Lilly LM, *et al.* Neutrophils produce interleukin 17A (IL-17A) in a dectin-1- and IL-23-dependent manner during invasive fungal infection. *Infect Immun* 2011; **79:** 3966–3977.
31. Kumar N, Kojetin DJ, Solt LA, *et al.* Identification of SR3335 (ML-176): a synthetic RORalpha selective inverse agonist. *ACS Chem Biol* 2011; **6:** 218–222.
32. Giguere V, Beatty B, Squire J, *et al.* The orphan nuclear receptor ROR alpha (RORA) maps to a conserved region of homology on human chromosome 15q21–q22 and mouse chromosome 9. *Genomics* 1995; **28:** 596–598.
33. Dzhagalov I, Giguere V, He YW. Lymphocyte development and function in the absence of retinoic acid-related orphan receptor alpha. *J Immunol* 2004; **173:** 2952–2959.
34. Pozo D, Garcia-Maurino S, Guerrero JM, *et al.* mRNA expression of nuclear receptor RZR/RORalpha, melatonin membrane receptor MT, and hydroxindole-O-methyltransferase in different populations of human immune cells. *J Pineal Res* 2004; **37:** 48–54.
35. Soria V, Martinez-Amoros E, Escaramis G, *et al.* Differential association of circadian genes with mood disorders: CRY1 and NPAS2 are

associated with unipolar major depression and CLOCK and VIP with bipolar disorder. *Neuropsychopharmacology* 2010; **35:** 1279–1289.
36. Dehghan A, Dupuis J, Barbalic M, *et al.* Meta-analysis of genome-wide association studies in >80 000 subjects identifies multiple loci for C-reactive protein levels. *Circulation* 2011; **123:** 731–738.
37. Chambers JC, Zhang W, Sehmi J, *et al.* Genome-wide association study identifies loci influencing concentrations of liver enzymes in plasma. *Nature Genet* 2011; **43:** 1131–1138.
38. Moffatt MF, Gut IG, Demenais F, *et al.* A large-scale, consortium-based genomewide association study of asthma. *N Engl J Med* 2010; **363:** 1211–1221.
39. Wong SH, Walker JA, Jolin HE, *et al.* Transcription factor RORalpha is critical for nuocyte development. *Nature Immunol* 2012; **13:** 229–236.
40. Dzhagalov I, Zhang N, He YW. The roles of orphan nuclear receptors in the development and function of the immune system. *Cell Mol Immunol* 2004; **1:** 401–407.
41. Wipke BT, Allen PM. Essential role of neutrophils in the initiation and progression of a murine model of rheumatoid arthritis. *J Immunol* 2001; **167:** 1601–1608.
42. Amelink M, de Groot JC, de Nijs SB, *et al.* Severe adult-onset asthma: a distinct phenotype. *J Allergy Clin Immunol* 2013; **132:** 336–341.
43. Karsten CM, Pandey MK, Figge J, *et al.* Anti-inflammatory activity of IgG1 mediated by Fc galactosylation and association of FcγRIIB and dectin-1. *Nature Med* 2012; **18:** 1401–1406.
44. Samavedam UK, Kalies K, Scheller J, *et al.* Recombinant IL-6 treatment protects mice from organ specific autoimmune disease by IL-6 classical signalling-dependent IL-1ra induction. *J Autoimmun* 2013; **40:** 74–85.
45. Hirose M, Vafia K, Kalies K, *et al.* Enzymatic autoantibody glycan hydrolysis alleviates autoimmunity against type VII collagen. *J Autoimmun* 2012; **39:** 304–314.
46. Kulkarni S, Sitaru C, Andersson KE, *et al.* Essential role for PI3Kβ in neutrophil activation by immune complexes. *Sci Signal* 2011; **4**: ra23.
47. Darby C, Geahlen RL, Schreiber AD. Stimulation of macrophage Fc gamma RIIIA activates the receptor-associated protein tyrosine kinase Syk and induces phosphorylation of multiple proteins including p95Vav and p62/GAP-associated protein. *J Immunol* 1994; **152:** 5429–5437.
48. Raichur S, Fitzsimmons RL, Myers SA, *et al.* Identification and validation of the pathways and functions regulated by the orphan nuclear receptor, ROR alpha1, in skeletal muscle. *Nucleic Acids Res* 2010; **38:** 4296–4312.
49. Lau P, Nixon SJ, Parton RG, *et al.* RORalpha regulates the expression of genes involved in lipid homeostasis in skeletal muscle cells: caveolin-3 and CPT-1 are direct targets of ROR. *J Biol Chem* 2004; **279:** 36828–36840.
50. Lee JM, Kim IS, Kim H, *et al.* RORα attenuates Wnt/β-catenin signaling by PKCα-dependent phosphorylation in colon cancer. *Mol Cell* 2010; **37:** 183–195.
51. Chiriac MT, Roesler J, Sindrilaru A, *et al.* NADPH oxidase is required for neutrophil-dependent autoantibody-induced tissue damage. *J Pathol* 2007; **212:** 56–65.